IOP Publishing Physica Scripta
Phys. Scr. 93 (2018) 024002 (10pp) https://doi.org/10.1088/1402-4896/aa95eb

Influence of sulfurization temperature on Cu_2ZnSnS_4 absorber layer on flexible titanium substrates for thin film solar cells

Dilara Gokcen Buldu[1], Ayten Cantas[1], Fulya Turkoglu[1], Fatime Gulsah Akca[1], Ece Meric[1], Mehtap Ozdemir[1,2], Enver Tarhan[1], Lutfi Ozyuzer[1,2] and Gulnur Aygun[1]

[1] Department of Physics, Izmir Institute of Technology, Urla, 35430, Izmir, Turkey
[2] Teknoma Technological Materials Inc., Izmir Technology Development Zone, Urla, 35430, Izmir, Turkey

E-mail: gulnuraygun@iyte.edu.tr

Received 26 April 2017, revised 25 September 2017
Accepted for publication 25 October 2017
Published 8 January 2018

Abstract

In this study, the effect of sulfurization temperature on the morphology, composition and structure of Cu_2ZnSnS_4 (CZTS) thin films grown on titanium (Ti) substrates has been investigated. Since Ti foils are flexible, they were preferred as a substrate. As a result of their flexibility, they allow large area manufacturing and roll-to-roll processes. To understand the effects of sulfurization temperature on the CZTS formation on Ti foils, CZTS films fabricated with various sulfurization temperatures were investigated with several analyses including x-ray diffraction (XRD), scanning electron microscopy (SEM), x-ray photoelectron spectroscopy and Raman scattering. XRD measurements showed a sharp and intense peak coming from the (112) planes of the kesterite type lattice structure (KS), which is strong evidence for good crystallinity. The surface morphologies of our thin films were investigated using SEM. Electron dispersive spectroscopy was also used for the compositional analysis of the thin films. According to these analysis, it is observed that Ti foils were suitable as substrates for the growth of CZTS thin films with desired properties and the sulfurization temperature plays a crucial role for producing good quality CZTS thin films on Ti foil substrates.

Keywords: Cu_2ZnSnS_4 thin film, flexible substrate, magnetron sputtering, sulfurization temperature

(Some figures may appear in colour only in the online journal)

1. Introduction

Cu_2ZnSnS_4 (CZTS) is one of the most promising candidate materials among many others as an absorber layer for solar cells. Since CZTS does not contain any rare elements, like Ga and In, and any toxic elements such as Cd, it is an excellent candidate for replacing the conventional $Cu(In,Ga)Se_2$ (CIGS) and CdTe thin film solar cells.

CZTS is a p-type semiconductor with a large absorption coefficient (larger than $10^4\,cm^{-1}$) having a direct bandgap at around 1.5 eV [1]. This property makes it a superior candidate to many others as an absorber layer in solar cell devices especially for the replacement of conventional Si whose bandgap is indirect and, therefore, limiting its performance [2]. Recently, the best efficiency of a CZTSSe solar cell produced with a hydrazine-based solution in a non-vacuum environment is reported to be 12.6% [3] and the best reported value for a CZTS solar cell produced with a two-layer CZTS absorber in vacuum-based method is 9.4% [4].

Several methods have been used for the fabrication of a CZTS thin film absorber layer such as electrodeposition [5, 6], spray pyrolysis deposition [7], hydrazine-based solution [3], co-evaporation [8], and magnetron sputtering [9–13]. Most of these techniques use a rigid substrate such as molybdenum (Mo) coated soda lime glass (SLG) which restricts the area of applications. This limitation can be

avoided with the use of flexible substrates. In fact, it is possible to produce thin film solar cells fabricated on flexible substrates such as aluminum (Al), molybdenum (Mo), stainless steel (SS) foils. The flexibility of these solar cells plays a major role to reduce the total thickness of the films and their cost as well. There are already some reports of CZTS thin films on flexible substrates [9, 14–16]. The highest reported conversion efficiency for such a thin film grown by electrodeposition method on Mo foil substrate is 3.82% [14]. However, the conversion efficiencies of flexible CZTS thin film solar cells are still lower than those of the rigid CZTS thin film solar cells [3]. Therefore, there is a need for more research to understand the growth mechanism of CZTS thin films on flexible substrates and to improve their efficiencies beyond those of conventional rigid ones.

Improvements in efficiency values of CZTS solar cells can be achieved in several ways. Especially, reductions in the impurity and defect concentrations can help to improve the conversion efficiency. Defect concentrations can be lowered using vacuum or low pressure growth techniques such as magnetron sputtering which is also our choice for the growth method in this study. Since the study of sputtered CZTS thin films on flexible substrates is still new, there are only few works using Ti [9], Mo [9, 15], Al and SS foils [16]. Another important issue affecting the performance is the choice of back contact material. The interface between back contact and absorber layer is also important in terms of minority charge carrier transportation. Therefore, back contact material should be chemically inert. The thermal expansion coefficient of the foil substrate and the absorber layer should also be in the same range [17–19].

During the deposition of CZTS thin films on flexible substrates, several defects may be formed. Crack formation on Mo foil [9], secondary phase formation on Al foil and FeS interface layer on SS foil [16] are some of the examples to defect formation during the deposition of CZTS thin films on flexible substrates. In this study, a Ti foil substrate was chosen as the substrate considering the results of our previous work [9] in which no crack formation was observed in the CZTS thin films grown on Ti foils. This is mainly because of the accordance of thermal expansion coefficients of Ti foil and CZTS absorber [9]. Moreover, not any CZTS thin films growth studies on flexible Ti foils followed by various sulfurization temperatures (530–580 °C) has been reported in the literature yet.

The growth mechanism and the average grain size of CZTS thin films are also important for making an absorber layer resulting in high efficiency. The conversion efficiency of thin films is strongly related to the grain size due to the enhanced minority carrier diffusion lengths and built-in potentials in thin film solar cells [20]. Since the grain boundaries act as recombination centers, the presence of an excessive number of grains causes a drop in the open circuit voltage of the solar cells [21, 22]. In the two-step sulfurization method, the sulfurization temperature affects not only the secondary phase formation [23], but it also plays a major role in the grain size [24], i.e. the grains become larger with increasing sulfurization temperature [25].

2. Experimental methods

200 μm thick and 0.8 cm × 2.5 cm surface area Ti foil are used as substrates. Before sputtering, Ti substrates were chemically etched in a diluted HF acid mixed solution including 90.0 ml water and 10.0 ml HF for 1.5 min at room temperature to remove the oxide layer on it. After etching, the thickness of Ti substrate was about 150 μm. The precursor layers were deposited by a multi-target DC magnetron sputtering system using 2-inch targets of Cu (99.999%), Zn (99.99%), and Sn (99.999%) at room temperature. Each layer's thickness in the metallic precursor was calculated by considering the molecular weight and density of each element of a layer. The distance between the target and the substrate was fixed at 8 cm. Before sputtering, the pressure in the chamber was lowered down to 1.7×10^{-4} Pa using a turbo molecular pump (TMP). During the sputtering, pure argon gas with 30 standard cubic centimeter per minute (sccm) flowing rate was fed into the chamber and the working gas pressure was maintained at 2.0 Pa. The metallic precursor Cu/Sn/Zn layers were sequentially deposited on the flexible Ti substrate. Since Sn and Zn have low melting points, Cu layer was chosen as the top metallic layer to reduce the loss of these elements during the sulfurization. The magnetron sputtering method provides an easy control of layer thickness and composition of precursor [26]. The deposition power and duration for each layer were optimized by considering the stoichiometry reported in the literature for the most efficient CZTS based solar cells which have Zn-rich and Cu-poor nominal composition. The resulted power values were 41, 40 and 20 W for Cu, Sn and Zn, respectively. The thicknesses of precursor metallic layers were obtained as 126, 290 and 193 nm for Cu, Sn and Zn, respectively.

After the metallic precursors were deposited, the sulfurization process was carried out in a quartz tube having 2.6 cm diameter and 60 cm length. Before the sulfurization process, the quartz tube was cleaned using 150 sccm argon gas flow for 15 min 250 mg sulfur powder was placed in the middle of a graphite box, then, the metallic precursor was placed to cover the sulfur powder. After the lid of the graphite box was closed, it was placed in the middle of the quartz tube in the furnace. During the sulfurization process, pure argon gas of 47 sccm flowed throughout the quartz tube as a carrier and protective gas. The sulfurization process was carried at the atmospheric pressure. It took 15 min to reach to the desired sulfurization temperature. The sulfurization duration for all samples was kept constant for 20 min. The sulfurization temperature was varied from 530 to 580 °C from sample to sample. After the sulfurization process, the samples were naturally cooled down in Ar atmosphere. As a result of sulfurization of 600 nm thick metallic precursor, CZTS film with a thickness of approximately 1.5 μm was obtained.

The crystal structure of the CZTS thin films were analyzed by x-ray diffraction (XRD) using a Philipps X'Pert Pro Diffractometer. The XRD device was operated in the Bragg-Brentano focusing geometry from 20° to 80° with CuK_{α} radiation ($\lambda = 1.5406$ Å) using an angular step size of 0.03° at a time step of 1.1 s. Phonon modes of CZTS films were

studied by means of a confocal micro-Raman spectroscopy system (S&I Mono Vista) equipped with a 100 mW Melles-Griot Ar ion laser operating at 514.5 nm, an Olympus BX51 down-looking microscope with 5x, 10x, 50x, and 100x objectives, and a 750 mm focal length monochromator (Princeton Instrument, Acton SP2750 0.750 mm Imaging Triple Grating Monochromator) containing a turret of a triple grating set of 150, 600, and 1800 grooves/mm holographic gratings. Raman signal was collected with a high-resolution CCD camera having 1600 × 200 pixels. To be able to see the Raman active phonon modes of CZTS films and the vibrational modes of some other possible phases, 514.5 nm excitation wavelength is the best choice by considering the absorption coefficient of CZTS [27]. The CZTS thin film morphology was investigated using a scanning electron microscope (SEM; Phillips XL 30S FEG) equipped with energy dispersive spectroscopy (EDS; EDAX). SEM images were taken using a 15 kV acceleration voltage. EDS measurements were done using an EDX detector with HV resolution in 15 kV having 1000x magnification with scaling 20 μm in a high vacuum. The area of EDS analysis is 100 μm × 100 μm. EDS analysis was needed to determine the stoichiometry of the films. X-ray photoelectron spectroscopy (XPS; SPECS Phoibos 150 3D-DLD) analysis was carried out to determine the chemical states of the film surface. XPS measurements were performed with a monochromatized MgK_α radiation source ($h\nu = 1254$ eV) of 200 W and 1.5 kW. The pressure in the chamber was set to be between 10^{-7}–10^{-8} Pa. High resolution scans of each element existing CZTS were conducted at 30 eV pass energy with a scan rate of 0.05 eV s^{-1} for a 2 s dwell time. The spectra were calibrated with respect to C 1*s* line at 284.6 eV which is characteristic for aromatic/aliphatic carbons [28, 29]. For the analysis, a Shirley-type background was used and the curves were fitted with Gaussian/Lorentzian product (GL(p)) functions using CasaXPS software.

3. Results and discussion

3.1. The morphology of CZTS thin films on Ti substrate

Microstructural changes of sulfurized CZTS films were clearly observed in the tilted cross-sectional SEM images as seen in figure 1. According to the SEM images of the films sulfurized at 530 °C, the observed grains with small sizes and different shapes are probably due to the result of different phases present in the films and incomplete crystallization of the CZTS phase. ZnS and Cu_2SnS_3 phases react with a chemical reaction to form CZTS phase formation [30]. According to the Schurr *et al* ZnS and Cu_2SnS_3 phases occur at around 537 °C and the kesterite crystallization starts upon reaching to this temperature (537 °C) and is completed around 572 °C. Therefore, it is possible to think that the films sulfurized at 530 and 540 °C may not able to complete the crystallization process and might have different phases. Over 540 °C, the grain sizes become larger and also in a densely packing because of the enhanced crystallization. Therefore, the grains coalesce to form CZTS structure above 540 °C. However, it is observed that the grain sizes reduce at about 580 °C. It can be thought that this could be the result of decomposition of CZTS [31, 32]. The film morphology and crystallinity become more uniform and denser between 550–570 °C. Therefore, it can be suggested that these sulfurization temperatures might be more applicable to the fabrication of CZTS absorber layer.

3.2. Structural properties

Figure 2 shows normalized XRD patterns of thin films sulfurized at different temperatures. The peaks located at $2\theta = 23.33$, 28.47, 29.95, 32.99, 44.96, 47.33, 56.18, 58.95, 69.23 and 76.45° correspond to (110), (112), (103), (200), (105), (220), (312), (224), (008) and (332) planes, respectively. The observed XRD patterns match quite well with the standard XRD pattern of kesterite Cu_2ZnSnS_4 (JCPDS 26-0575), indicating the formation of kesterite CZTS for all sulfurization temperatures. However, there occurred a slight shift in the positions of (112) peak, which is the characteristic peak corresponding to kesterite CZTS structure. These types of shifts in the position of the diffraction peaks can occur due to internal strain. Position of the peaks can be shifted toward lower 2θ for the case of tensile stress or toward higher 2θ for the compressive stress. Moreover, stress in the films can affect the distances between the atomic planes resulting in a shift of the peaks in XRD. Furthermore, non-stoichiometry of the formed structure or applied sulfurization temperature and/or impurities could cause these types of peak shifts in XRD characterization. Some reported works showed that XRD peaks are shifted toward lower 2θ as a result of increasing temperature [33]. However, it was not observed a significant trend with the sulfurization temperature during the course of this work. Thus, it is not suitable to say that this shift is directly related to the sulfurization temperature. Therefore, it is thought that the peak shift observed in the films could be the result of impurities. Moreover, the peaks located at $2\theta = 38.31$, 40.13, 52.93 and 70.94° come from the Ti substrate (JCPDS: 00-044-1294). As it can be seen given in the literature, CZTS films having additional peaks at $2\theta = 27.34$, 36.12 and 54.47° confirm the presence of the titanium rutile phase (JCPDS: 00-044-1294).

Some weak impurity peaks were detected in addition to the ones belonging to the kesterite CZTS and Ti substrate. The peak detected at 31.6° was probably originated from (033) diffraction plane of monoclinic Cu_2S (JCPDS: 01-083-1462). Another impurity peak detected at 32.1° corresponds to (200) diffraction plane of cubic Cu_2S (JCPDS: 00-053-0522). For the CZTS films sulfurized at 530 and 540 °C, additional impurity peak of SnS_2 (JCPDS: 00-040-1466) was detected at 52.9° and 53.1°. Although some secondary phases were observed for the samples sulfurized below 550 °C, no secondary phases were detected above 550 °C sulfurization temperature.

Moreover, ZnS (JCPDS: 00-05-0566) and Cu_2SnS_3 (JCPDS: 00-027-0198) secondary phases have very similar crystal structures with the kesterite CZTS. For this reason,

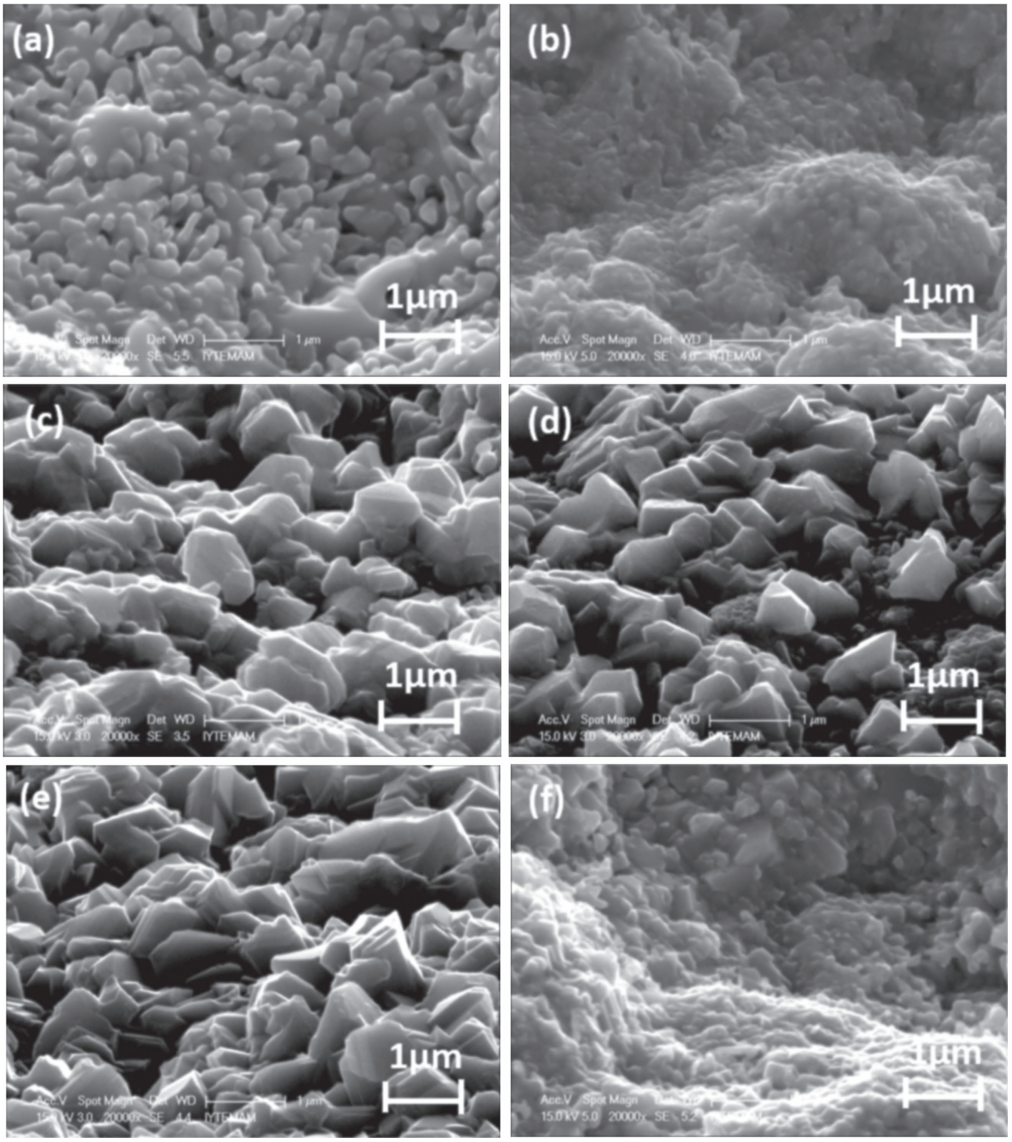

Figure 1. Tilted SEM images of CZTS thin films on Ti foil for (a) 530 °C, (b) 540 °C, (c) 550 °C, (d) 560 °C, (e) 570 °C, and (f) 580 °C sulfurization temperatures.

XRD analysis is not alone enough to determine whether the structure is kesterite or not (JCPDS: 026-0575). Therefore, Raman analysis is required to define from which the signal is resulted. Therefore, these absorbers were further examined by the Raman scattering measurements.

Figure 3 shows a series of Raman spectra of thin films. Each Raman spectrum is the average of measurements taken from four different places on each sample. All of these four measurements show similar spectra indicating the homogeneity of our films. As seen in figure 3, the characteristic Raman peaks of Cu_2ZnSnS_4 are nearly at 252, 289, 335-337, and 374 cm^{-1} [34–37], indicating the formation of kesterite structure of the films. Weak peak observed at around 266 cm^{-1} corresponds to kesterite CZTS [38]. The other weak peak detected at 470 cm^{-1} belongs the Cu_2S secondary phase which was observed for sulfurized films at 530, 550 and 580 °C. This phase, however, was not detected in XRD measurement of the CZTS film sulfurized at 580 °C, which may be due to the detection limit of the XRD device. As in XRD analyses, Raman measurements also confirmed that 570 °C can be defined as the best sulfurization temperature for CZTS films on Ti foil substrates.

3.3. Composition of CZTS thin films

CZTS formation requires a systematic control of sputtering conditions. Deposition for a desired thickness of a metallic layer is realized by changing the sputtering duration and applied power. Thickness of each sublayer out of three plays a crucial role in the formation of CZTS structure. Sulfurization temperature and duration also play a significant role in the formation of CZTS compound. Elemental analysis in the CZTS composition was done by carrying out EDS measurements. Table 1 lists the atomic percentages of each element, as well as Zn/Sn and Cu/(Zn+Sn) ratios for different sulfurization temperatures. Furthermore, structural quality and stoichiometry play a key role in the solar cell performances.

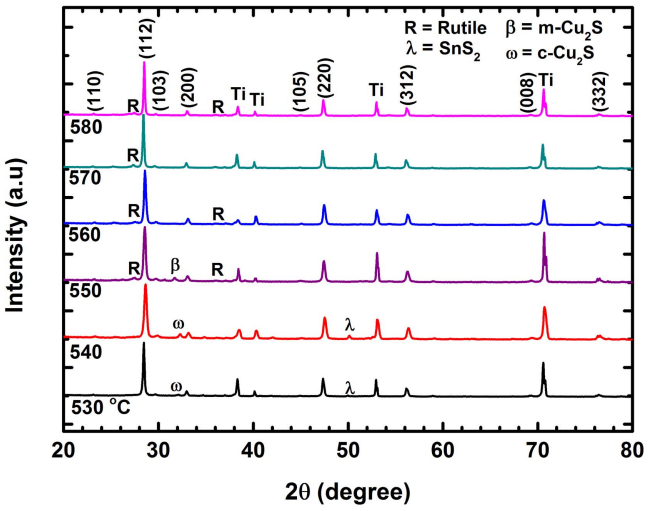

Figure 2. Normalized XRD patterns of CZTS thin films on Ti foils sulfurized at (a) 530 °C, (b) 540 °C, (c) 550 °C, (d) 560 °C, (e) 570 °C and (f) 580 °C.

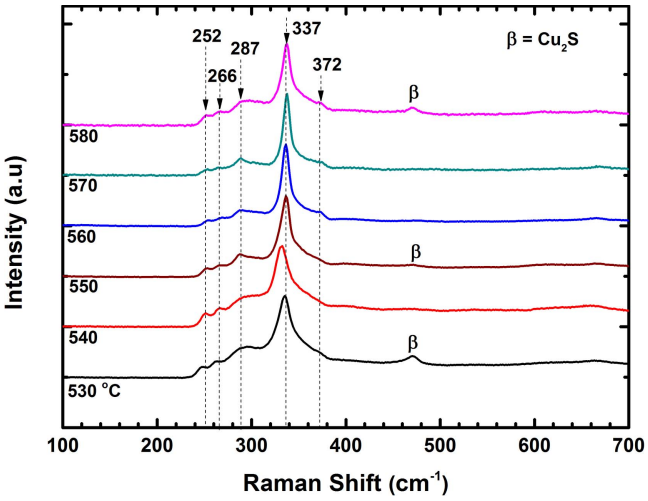

Figure 3. Raman spectra of CZTS thin films on Ti foils for the sulfurization temperatures of (a) 530 °C, (b) 540 °C, (c) 550 °C, (d) 560 °C, (e) 570 °C and (f) 580 °C.

Reported studies show that CZTS films with Cu-poor (Cu/(Zn+Sn) ~ 0.8–0.9) and Zn-rich (Zn/Sn ~ 1.1–1.2) compositions have better device performances resulting in higher cell efficiencies [2, 39–43] since the Cu-poor composition enhances the formation of Cu vacancies (V_{Cu}) acting as acceptor-like point defects and increasing p-type conductivity [44].

In this study, the sulfurized films at 540–580 °C have similar elemental ratios to those reported in the literature. However, the sulfurized at 530 °C one has a considerably higher Zn/Sn ratio than the reported ones. The higher amount of Zn in the defined film may indicate the presence of ZnS phase in the CZTS structure. Furthermore, CZTS is self-doped of intrinsic defects throughout the formation stage. The defects at the cationic substitution sites are related to non-stoichiometry [45–47]. According to Valle Rios *et al* four types of point defects are possible when atomic composition of constituent elements are considered [47]. In our case, thin films grown at 530 °C and 550 °C showed Cu-poor/Zn-rich/Sn-poor composition (B-type formation) while sulfurized thin films at 540 °C and 560 °C have a Cu-rich/Zn-poor/Sn-rich compositions (C-type formation). At sulfurization temperature of 570 and 580 °C cases, Cu-poor/Zn-rich/Sn-constant composition was seen in A-type formation. These compositions are suitable for device applications.

3.4. Chemical properties

XPS analysis is used to identify the surface chemical states of the constituting elements in a material, *i.e.*, CZTS films here. After obtaining XPS spectra, curve fitting analysis was realized to define the composition of the films. Moreover, since this technique uses the L-S coupling effect, other than *s* states, all *p* and *d* bands are doublets as $p_{3/2}$, $p_{1/2}$ and $d_{5/2}$, $d_{3/2}$, respectively.

Figure 4 shows a series of XPS spectra for the constituent elements *i.e.*, Zn 2*p,* Cu 2*p*, Sn 3*d*, and S 2*p* bands. The results of the curve fitting analysis for the observed peak positions are given in table 2. During peak fitting, spin–orbit splitting energies for each element were chosen as constant obtained from literature. More than one doublet attributing to different chemical states were detected in the XPS analysis of Cu 2*p*, Sn 3*d* and S 2*p* spectrum of some CZTS films. Therefore, the second column signifies the component of the second doublet of the same element, listed in table 2.

The signs of the chemical shifts during a bonding process indicate transferring of electrons and, therefore, resulting in a net exchange charge [48]. However, little to no shift in the binding energies for the same element was observed in different CZTS films. Hence, we conclude that any charge transfer does not occur indicating no phase changes in the formation.

Figure 4(a) shows the Zn 2*p* spectra of the films with respect to different sulfurization temperatures. The peak was fitted using a GL (80) function where 23.0 eV spin–orbit splitting energy was used. Zn $2p_{3/2}$ band spanning the spectral region from 1021.6 to 1022.3 eV according to the literature [49, 50] was also observed in our samples between 1021.8–1022.2 eV, which indicates +2 charge state for Zn in CZTS.

Figure 4(b) corresponds to Cu 2*p* band. The curve fitting using GL (90) and a spin–orbit splitting energy of 19.8 eV were used for this spectrum. For the films sulfurized at a temperatures higher than 550 °C, the 2*p* band consists of two doublets. In the first doublet band, two Cu $2p_{3/2}$ peaks were observed at about 932.0 eV which is an evidence for Cu^{1+} charge state in CZTS [50, 51]. In the Cu 2*p* spectra of films with sulfurization temperatures higher than 540 °C, the well-known shake up satellite shoulder is also seen between 940.0–945.0 eV, indicating Cu (II) bonds. It is reported in the literature that these bonds are due to sulfur oxide formations on the surface [52]. The existence of CuO phase was supported by the second doublet seen in the Cu 2*p* spectra. The second Cu $2p_{3/2}$ band observed between 933.2–934.8 eV energy range shows a CuO formation on the CZTS surface which was displayed by the samples with sulfurization

Table 1. EDS analyses for the atomic percentages of the constituent elements and some component ratios of the sulfurized CZTS thin films formed on Ti foil substrate.

Sample Name	Temperature (°C)	Cu (atomic%)	Zn (atomic%)	Sn (atomic%)	S (atomic%)	Zn/Sn	Cu/(Zn+Sn)	S/Metal
A	530	23.83	20.25	11.46	44.46	1.76	0.75	0.80
B	540	29.41	15.20	12.74	42.65	1.20	1.04	0.74
C	550	26.30	17.07	12.57	44.06	1.36	0.88	0.78
D	560	27.39	14.01	12.74	45.86	1.09	1.02	0.85
E	570	27.12	16.14	12.69	44.06	1.27	0.94	0.78
F	580	27.34	16.87	12.08	43.71	1.38	0.94	0.78

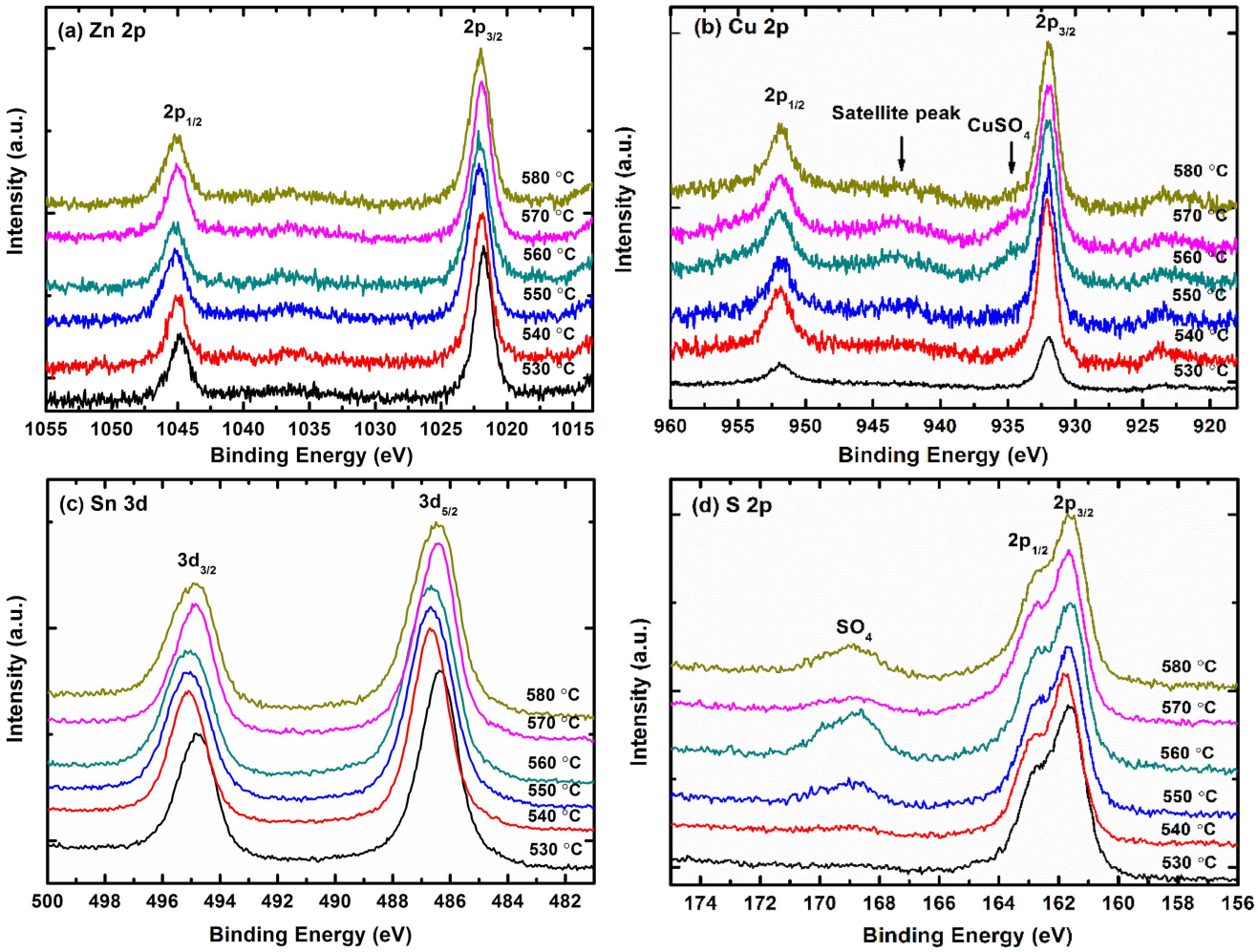

Figure 4. High-resolution XPS spectra of (a) Zn 2*p*, (b) Cu 2*p*, (c) Sn 3*d* and (d) S 2*p* bands.

Table 2. Curve fitting results for high resolution XPS spectra.

Sulfurization Temperature (°C)	Zn $2p_{3/2}$ (eV)	Cu $2p_{3/2}$ (eV)	Cu $2p_{3/2}$ (eV)	Sn $3d_{5/2}$ (eV)	Sn $3d_{5/2}$ (eV)	S $2p_{3/2}$ (eV)	S $2p_{3/2}$ (eV)
580 °C	1022.1	932.0	933.5	486.5	—	161.6	163.6
570 °C	1021.9	932.0	934.8	486.4	—	161.6	163.5
560 °C	1022.1	932.0	934.7	486.4	—	161.6	163.3
550 °C	1022.1	932.0	933.2	486.7	—	161.6	163.5
540 °C	1022.0	932.1	—	486.7	488.2	161.7	163.5
530 °C	1021.8	931.9	—	486.4	487.1	161.6	163.6

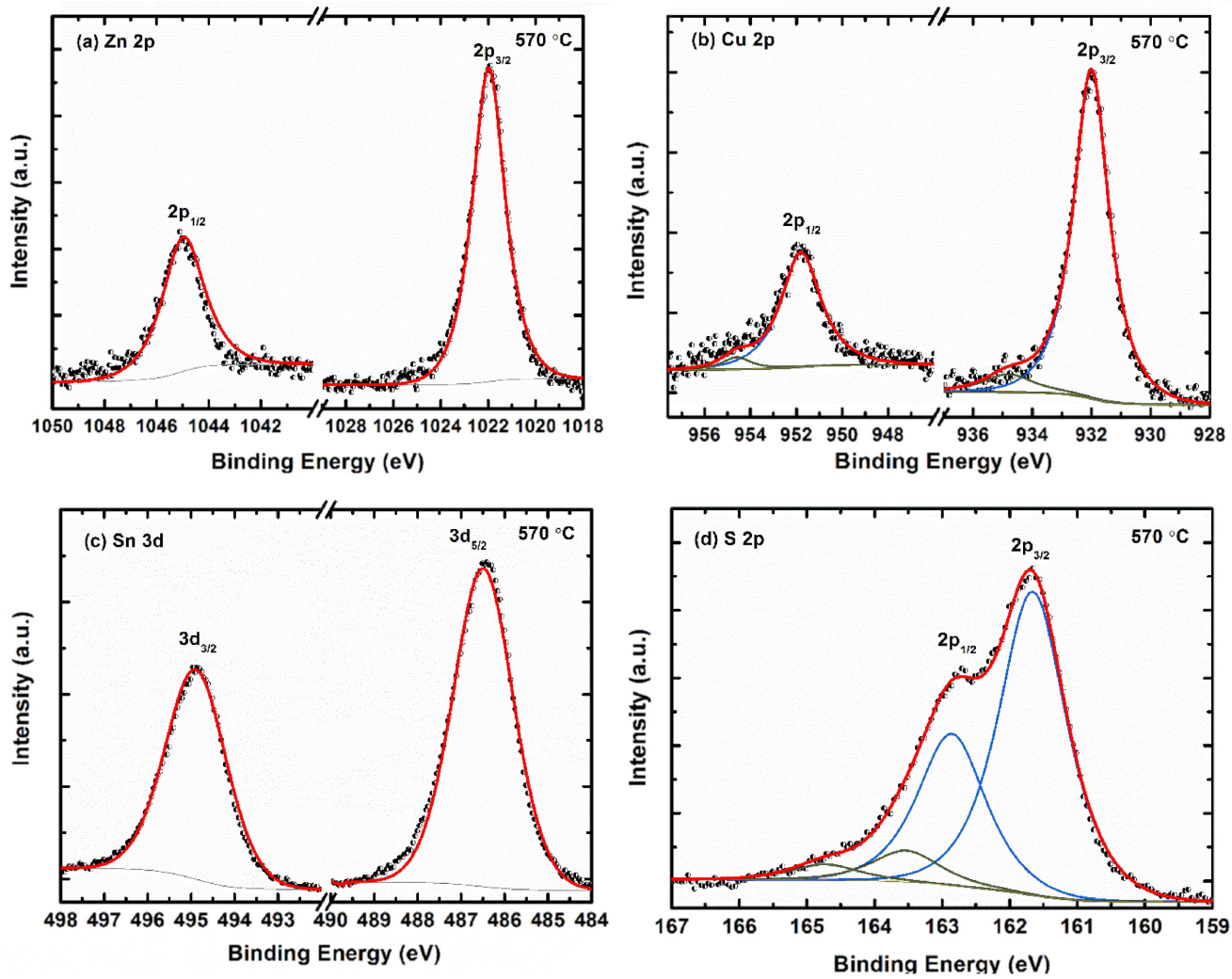

Figure 5. The detailed peak fitting analyses for the CZTS film sulfurized at 570 °C.

temperatures higher than 550 °C [52, 53]. The Cu $2p_{3/2}$ band of the samples with sulfurization temperatures higher than 550 °C exhibit a shoulder at 935.0–935.5 eV resulting from $CuSO_4$ formation [52].

Actually, etching with an Ar^+ ion beam is generally needed to remove the contaminations and/or oxide phases from the film's surface. However, it may result in the degradation of chemical state of the surface [28] and/or damage to the surface of the film. For these reasons, during the course of this work, Ar^+ etching process was not applied to the surface of CZTS films before XPS measurements. Therefore, we can clearly attribute to the CuO and $CuSO_4$ phases in the detected Cu 2*p* peaks.

XPS spectra of the Sn 3*d* bands are given in figure 4(c). Each band shows one or two couples of peaks which were fitted by means of GL (35) function and a spin–orbit splitting energy of 8.4 eV. For all CZTS films, the Sn $3d_{5/2}$ band displays a couple of peaks between 486.3–486.6 eV energy range. These were assigned to the Sn (IV) state in CZTS [50, 51]. The Sn 3*d* spectra of the CZTS films with sulfurization temperatures of 530 and 540 °C displays a second couple at 487.8 and 488.4 eV energies. Shin *et al* indicates that the Sn $3d_{5/2}$ peak observed at 487.0 eV is due to Sn in SnS_2 phase [49]. Cruz *et al* attributed the peaks at 487.1 and 488.2 eV to SnS and Sn_2S_3 phases, respectively [54]. Yang *et al* proposed that the Sn $3d_{5/2}$ peaks at 487.2 and 488.3 eV are due to SnS and SnS_2, respectively [55]. Thus, it can be said that there exists Sn based secondary phase formations in our samples and these results are consistent with the XRD and Raman analysis of the same CZTS films with the sulfurization temperatures of 530 and 540 °C.

XPS spectra for S 2*p* state of CZTS films can be seen in figure 4(d). Each spectrum consists of two doublets with a spin–orbit splitting energy of 1.2 eV. GL (75) function was used during the peak fitting analysis of S 2*p* state. While $2p_{3/2}$ band observed at a peak position of 161.7 or 161.6 eV represents an expected monosulfide phase (S^{2-}), the second $2p_{3/2}$ band observed at a peak position between 163.3 and 163.6 eV for all samples corresponds to a surface polysulfide phase [50, 56]. This phase, generally detected in the range of 163.4 eV [57] and 163.8 eV [58], can be traced from the literature.

All CZTS films except the ones corresponding to the sulfurization temperatures of 530 and 540 °C contain another

bonding state of sulfur at a higher binding energy region (168.8 eV). This result implies the formation of copper sulfate ($CuSO_4$) as inferred from the Cu 2*p* peak analysis (figure 4(b)). Moreover, as mentioned above, the observed $CuSO_4$ phase may relate to the bonding between CuO and S in an oxidized CZTS surface. While CZTS films sulfurized at 580, 560 and 550 °C demonstrate a strong $CuSO_4$ formation, the films sulfurized at 570 °C show almost none.

The detailed plotting for the peak fitting analyses of the film sulfurized at 570 °C film is given in figures 5(a)–(d). When all of our CZTS films with different sulfurization temperatures are considered as a candidate for the solar cell absorber layer, the film sulfurized at the 570 °C is the most favorable one since it shows few secondary phases with very little sulfate formation.

4. Conclusion

CZTS films on Ti flexible substrates were fabricated by a two-step process. The first step is the formation of Cu, Sn and Zn layers, respectively, on flexible Ti folio substrates by using magnetron sputtering technique. The second step is the sulfurization of these precursor layers in a tubular furnace at varied applied temperatures. The effect of the sulfurization temperature on the morphology, composition and structural properties of CZTS thin films produces on Ti flexible substrates was investigated by means of SEM, Raman, XRD, EDS and XPS techniques.

The deduced results of SEM images showed that all CZTS thin films had compact and dense surfaces without having any cracks on the films. Furthermore, neither void formation nor degradation were observed in the SEM images of these films. It was observed that from the SEM images that the grain sizes became larger with respect to increasing sulfurization temperatures, up to 570 °C, then they started to become smaller. Since large grain size is a desired quality for a better conductivity in an absorber layer of a solar cell, the knowledge of the best sulfurization temperature is very important for the production of good quality absorber layers. Therefore, it can be concluded that the best candidate for a CZTS absorber layer is the one sulfurized at 570 °C.

XRD and Raman analysis also showed that the crystal structure of the CZTS thin film produced at the sulfurization temperature of 570 °C had almost a single phase although some secondary phases were hardly visible. EDS results of these films indicate that a Cu-poor/Zn-rich composition, desired as well for solar cell applications, were obtained at the sulfurization temperature of 570 °C. XPS spectra of the CZTS film sulfurized at 570 °C show that the film sulfurized at 570 °C does not contain any considerable amount of secondary phases on or near the surface. This result is also consistent with XRD and Raman analysis. Moreover, this conclusion can be extended, not only to the surface of the film, but also to the deeper layers, since XRD and Raman data are obtained from the deeper levels of the film.

Finally, it can be said that producing and characterizing the absorbing layer of solar cells is a highly important process in terms of renewable energy. Production of CZTS thin films on Ti flexible foils is a current and important research area since it enables humanity to produce a flexible, and hence, better durable solar cells at lower costs for a widespread industrial application. Therefore, the results of this research provide a highly important step in the industrial application stage.

Acknowledgments

This research was supported by The Scientific and Technological Research Council of Turkey (TUBITAK) with the project number of 114F341 and Applied Quantum Research Center (AQuRec).

References

[1] Katagiri H, Sasaguchi N, Hando S, Hoshino S, Ohashi J and Yokota T 1997 Preparation and evaluation of Cu_2ZnSnS_4 thin films by sulfurization of E-B evaporated precursors *Sol. Energy Mater. Sol. Cells* **49** 407

[2] Todorov T K, Reuter K B and Mitzi D B 2010 High-efficiency solar cell with earth-abundant liquid-processed absorber *Adv. Mater.* **22** E156–9

[3] Wang W, Winkler M T, Gunawan O, Gokmen T, Todorov T K, Zhu Y and Mitzi D B 2014 Device characteristics of CZTSSe thin-film solar cells with 12.6% efficiency *Adv. Energy Mater.* **4** 1301465

[4] Tajima S, Umehara M, Hasegawa M, Mise T and Itoh T 2017 Cu_2ZnSnS_4 photovoltaic cell with improved efficiency fabricated by high-temperature annealing after CdS buffer-layer deposition *Prog. Photovolt., Res. Appl.* **25** 14–22

[5] Scragg J, Dale P J and Peter L M 2008 Towards sustainable materials for solar energy conversion: preparation and photoelectrochemical characterization of Cu_2ZnSnS_4 *Electrochem. Commun.* **10** 639

[6] Ennaoui A *et al* 2009 Cu2ZnSnS4 thin film solar cells from electroplated precursors: novel low-cost perspective *Thin Solid Films* **517** 2511

[7] Yoo H and Kim J 2011 Comparative study of Cu_2ZnSnS_4 film growth *Sol. Energy Mater. Sol. Cells* **95** 239

[8] Tanaka T, Yoshida A, Saiki D, Saito K, Guo Q, Nishio M and Yamaguchi T 2010 Influence of composition ratio on properties of Cu_2ZnSnS_4 thin films fabricated by co-evaporation *Thin Solid Films* **518** 29–33

[9] Yazici S, Olgar M A, Akca F G, Cantas A, Kurt M, Aygun G, Tarhan E, Yanmaz E and Ozyuzer L 2016 Growth of Cu_2ZnSnS_4 absorber layer on flexible metallic substrate for thin film solar cell applications *Thin Solid Films* **589** 563

[10] Jimbo K, Kimura R, Kamimura T, Yamada S, Mav W S, Araki H, Oishi K and Katagiri H 2007 Cu_2ZnSnS_4-type thin film solar cells using abundant materials *Thin Solid Films* **515** 5997

[11] Ericson T, Kubbart T, Scragg J J and Platzer-Björkman C 2012 Reactive sputtering of precursors for Cu_2ZnSnS_4 thin film solar cells *Thin Solid Films* **520** 7093

[12] Liu F, Li Y, Zhang K, Wang B, Yan C, Lai Y, Zhang Z, Lie J and Lu Y 2010 *In situ* growth of Cu_2ZnSnS_4 thin films by reactive magnetron co-sputtering *Sol. Energy Mater. Sol. Cells* **94** 2431

[13] Fernandes P A, Salome P M P and da Cunha A F 2009 Growth and Raman scattering characterization of Cu_2ZnSnS_4 thin films *Thin Solid Films* **517** 2519

[14] Zhang Y, Ye Q, Liu J, Chen H, He X, Liao C, Han J F, Wang H, Mei J and Lau W M 2014 Earth-abundant and low-cost CZTS solar cell on flexible molybdenum foil *RSC Adv.* **4** 23666
[15] Khalil M I, Atici O, Lucotti A, Binetti S, Le Donnec A and Magagnina L 2016 CZTS absorber layer for thin film solar cells from electrodeposited metallic stacked precursors (Zn/Cu-Sn) *Appl. Surf. Sci.* **379** 91
[16] Xu J, Cao Z and Yang Y 2015 Characterization of Cu_2ZnSnS_4 thin films on flexible metal foils *J. Mater. Sci: Mater Electron* **26** 726
[17] Scragg J J, Kubart T, Watjen J T, Ericson T, Linnarsson M K and Platzer-Björkman C 2013 Effects of back contact instability on Cu_2ZnSnS_4 devices and process *Chem. Mater.* **25** 3162
[18] Yang K J *et al* 2015 Effects of Na and MoS_2 on Cu_2ZnSnS_4 thin-film solar cell *Prog. Photovolt., Res. Appl.* **23** 862
[19] Yagioka T and Nakada T 2009 Cd-free flexible Cu(In, Ga)Se_2 thin film solar cells with ZnS(O,OH) buffer layers on Ti foils *Appl. Phys. Express* **2** 072201
[20] Pawar S M, Moholkar A V, Kim I K, Shin S W, Moon J H, Rhee J I and Kim J H 2010 Effect of laser incident energy on the structural, morphological and optical properties of Cu_2ZnSnS_4 (CZTS) thin films *Curr. Appl. Phys.* **10** 565
[21] Hegedus S S and Shafarman W N 2004 Thin-film solar cells: device measurements and analysis *Prog. Photovolt., Res. Appl.* **12** 155
[22] Li J, Mitzi D B and Shenoy V B 2011 Structure and electronic properties of grain boundaries in earth-abundant photovoltaic absorber Cu_2ZnSnS_4 *ACS Nano* **5** 8613
[23] Chalapathy R B V, Jung G S and Tae Ahn B 2011 Fabrication of Cu_2ZnSnS_4 films by sulfurization of Cu/ZnSn/Cu precursor layers in sulfur atmosphere for solar cells *Sol. Energy Mater. Sol. Cells* **95** 3216
[24] Pawar S M, Inamdar A I, Pawar B S, Gurav K V, Shin S W, Yanjun X, Kolekar S S, Lee J H, Kim J H and Im H 2014 Synthesis of Cu_2ZnSnS_4 (CZTS) absorber by rapid thermal processing (RTP) sulfurization of stacked metallic precursor films for solar cell applications *Mat. Lett.* **118** 76
[25] Sánchez T G, Mathew X and Mathews N R 2016 Obtaining phase-pure CZTS thin films by annealing vacuum evaporated CuS/SnS/ZnS stack *J. Cryst. Growth* **445** 15
[26] Subramanyam T K, Uthanna S and Srinivasulu Naidu B 1998 Influence of oxygen pressure on the structural and optical properties of DC magnetron reactive sputtered cadmium oxide films *Phys. Scr.* **57** 317–20
[27] Fernandes P A, Salomé P M P and da Cunha A F 2011 Study of polycrystalline Cu_2ZnSnS_4 films by Raman scattering *J. Alloys Compd.* **509** 7600
[28] Aygun G, Cantas A, Simsek Y and Turan R 2011 Effects of physical growth condition on the structural and optical properties of sputtered grown thin HfO_2 films *Thin Solid Films* **519** 5820–5
[29] Aygun G and Yildiz I 2009 Interfacial and structural properties of sputtered HfO2 layers *J. Appl. Phys.* **106** 014312
[30] Schurr R *et al* 2009 The crystallisation of Cu_2ZnSnS_4 thin film solar cell absorbers from Co-electroplated Cu-Zn-Sn precursors *Thin Solid Films* **517** 2465–8
[31] Chen G, Wang W, Zhang J, Chen S, Huang Z and Jian R 2017 Ultra-high sulfurization temperature drives the growth of oxide-derived Cu_2ZnSnS_4 thin film with very large grain *J. Renew. Sustain Ener.* **9** 013501
[32] Weber A, Mainz R and Schock H W 2010 On the Sn loss from thin films of the material system Cu–Zn–Sn–S in high vacuum *J. Appl. Phys.* **107** 013516
[33] Tsega M, Dejene F B and Kuo D-H 2015 Morphological evolution and structural properties of $Cu_2ZnSn(S,Se)_4$ thin films deposited from single ceramic target by a one-step sputtering process and selenization without H_2Se *J. Alloys Compd.* **642** 140–7
[34] Cormier P A and Snyders R 2015 One-step synthesis of Cu_2ZnSnS_4 thin films by reactive magnetron co-sputtering *Acta. Material* a **96** 80
[35] Valakh M Y *et al* 2013 Raman scattering and disorder effect in Cu_2ZnSnS_4 *Phys. Status Solidi RRL* **7** 258
[36] He J, Sun L, Chen Y, Jiang J, Yang P and Chu J 2014 Cu_2ZnSnS_4 thin film solar cell utilizing rapid thermal process of precursors sputtered from a quaternary target: a promising application in industrial processes *RSC Adv.* **4** 43080
[37] Guc M, Levcenko S, Bodnar I V, Izquierdo-Roca V, Fontane X, Volkova L V, Arushano E and Pérez-Rodríguez A 2016 Polarized Raman scattering study of kesterite type Cu_2ZnSnS_4 single crystals *Sci. Rep.* **6** 19414
[38] Cheng A J, Manno M, Khare A, Leighton C, Campbell S A and Aydil E S 2011 Imaging and phase identification of Cu_2ZnSnS_4 thin films using confocal Raman spectroscopy *J. Vac. Sci. Technol.* A **29** 051203
[39] Katagiri H, Jimbo K, Maw W S, Oishi K, Yamazaki M, Araki H and Takeuchi A 2009 Development of CZTS-based thin film solar cells *Thin Solid Films* **517** 2455
[40] Bjorkman C P, Scragg J, Flammersberger H, Kubart T and Edoff M 2012 Influence of precursor sulfur content on film formation and compositional changes in Cu_2ZnSnS_4 films and solar cells *Sol. Energy Mater. Sol. Cells* **98** 110
[41] Repins I, Beall C, Vora N, DeHart C, Kuciauskas D, Dippo P, To B, Mann J, Hsu W C and Goodrich A 2012 Co-evaporated $Cu_2ZnSnSe$ solar cells and devices *Sol. Energy Mater. Sol. Cells* **101** 154
[42] Shin B, Gunawan O, Zhu Y, Bojarczuk N A, Chey S J and Guha S 2013 Thin film solar cell with 8.4% power conversion efficiency using an earth-abundant Cu_2ZnSnS_4 absorber *Prog. Photovolt., Res. Appl.* **21** 72
[43] Todorov T, Gunawan O, Chey S J, de Monsabert T G, Prabhakar A and Mitzi D B 2011 Progress towards marketable Earth-abundant chalcogenide solar cells *Thin Solid Films* **519** 7378
[44] Chen S, Gong X G, Walsh A and Wei S 2010 Defect physics of the kesterite thin-film solar cell absorber Cu_2ZnSnS_4 *Appl. Phys. Lett.* **96** 021902
[45] Choubrac L, Lafond A, Guillot-Deudon C, Moelo Y and Jobic S 2011 Structure flexibility of the Cu_2ZnSnS_4 absorber in low-cost photovoltaic cells: from the stoichiometric to the copper poor compounds *Inorg. Chem.* **51** 3346–8
[46] Lafond A, Choubrac L, Guillot-Deudon C, Deniard P and Jobic S 2012 Crystal structures of photovoltaic chalcogenides, an intricate puzzle to solve: the cases of CIGSe and CZTS materials *Zeitschrift für Anorganische and Allgemeine Chemie* **638** 2571
[47] Valle Rios L E, Neldner K, Gurieva G and Schorr S 2016 Extistence of off-stoichiometric single phase kesterite *J. Alloys Compd.* **657** 408
[48] Moholkar A V, Shinde S S, Babar A R, Sim K U, Kwon Y, Rajpure K Y, Patil P S, Bhosale C H and Kim J H 2011 Development of CZTS thin films solar cells by pulsed laser deposition: influence of pulse repetition rate *Sol. Energy* **85** 1354
[49] Shin S W, Pawar S M, Park C Y, Yun J H, Moon J H, Kim J H and Lee J Y 2011 Studies on Cu_2ZnSnS_4 (CZTS) absorber layer using different stacking orders in precursor thin films *Sol. Energy Mater. Sol. Cells* **95** 3202
[50] Singh A, Geaney H, Laffir F and Ryan K M 2012 Colloidal synthesis of wurtzite Cu_2ZnSnS_4 nanorods and their perpendicular assembly *J. Am. Chem. Soc.* **134** 2910
[51] Das S, Frye C, Muzykov P G and Mandal K C 2012 Deposition and characterization of low-cost spray pyrolyzed

Cu_2ZnSnS_4 (CZTS) thin-films for large-area high-efficiency heterojunction *Solar Cells ECS Trans.* **45** 153

[52] Krylova V and Andrulevičius M 2009 Optical, XPS and XRD studies of semiconducting copper sulfide layers on a polyamide film *Int. J. Photoenergy* **2009** 304308

[53] Biesingera M C, Laua L W M, Gerson A R and Smart R 2010 Resolving surface chemical states in XPS analysis of first row transition metals, oxides and hydroxides: Sc, Ti, V, Cu and Zn *Appl. Surf. Sci.* **257** 887

[54] Cruz M, Morales J, Espinos J P and Sanz J 2003 XRD, XPS and 119Sn NMR study of tin sulfides obtained by using chemical vapor transport methods *J. Solid State Chem.* **175** 359

[55] Yang C, Qin M, Wang Y, Wan D, Huang F and Lin J 2013 Observation of an intermediate band in Sn-doped chalcopyrites with wide-spectrum solar response *Sci. Rep.* **3** 1286

[56] Acres R G, Harmer S L and Beattie D A 2010 Synchrotron XPS, NEXAFS, and ToF-SIMS studies of solution exposed chalcopyrite and heterogeneous chalcopyrite with pyrite *Int. J. Miner. Process.* **23** 928

[57] Acres R G, Harmer S L and Beattie D A 2010 Synchrotron XPS studies of solution exposed chalcopyrite, bornite, and heterogeneous chalcopyrite with bornite *Int. J. Miner. Process.* **94** 43

[58] Mikhlina Y L, Tomashevicha Y V, Asanovb I P, Okotrubb A V, Varnekb V A and Vyalikh D V 2004 Spectroscopic and electrochemical characterization of the surface layers of chalcopyrite ($CuFeS_2$) reacted in acidic solutions *Appl. Surf. Sci.* **225** 395